

# Process Parameters Optimization for Ultrasonically Consolidated Fiber-Reinforced Metal Matrix Composites

Y. Yang, G.D. Janaki Ram, and B.E. Stucker

Department of Mechanical and Aerospace Engineering, Utah State University

Logan, UT 84322-4130, USA

Reviewed, accepted September 14, 2006

## Abstract

As an emerging rapid prototyping technology, Ultrasonic Consolidation (UC) has been used to successfully fabricate metal matrix composites (MMC). The intent of this study is to identify the optimum combination of processing parameters, including oscillation amplitude, welding speed, normal force, operating temperature and fiber orientation, for manufacture of long fiber-reinforced MMCs. The experiments were designed using the Taguchi method, and an L25 orthogonal array was utilized to determine the influences of each parameter. SiC fibers of 0.1mm diameter were successfully embedded into an Al 3003 metal matrix. Two methods were employed to characterize the bonding between the fiber and matrix material: optical/electron microscopy and push-out tests monitored by an acoustic emission (AE) sensor. SEM images and data from push-out tests were analyzed and optimum combinations of parameters were achieved.

## 1. Introduction

Ultrasonic welding is one of the widely used solid-state welding processes [1,2]. Ultrasonic Consolidation (UC) is a novel rapid prototyping process recently developed by Solidica Inc., USA, implementing ultrasonic welding principles [3]. In this process (Fig.1), a rotating sonotrode travels along the length of a thin metal foil placed over the substrate. The thin foil is held closely in contact with the substrate by applying a normal force via the rotating sonotrode. The sonotrode oscillates transversely to the direction of welding at a frequency of 20 kHz and at a user-set oscillating amplitude, while traveling over the metal foil. The combination of normal and oscillating shear forces results in generation of dynamic interfacial stresses at the interface between the two mating surfaces [1-3]. The stresses produce elastic-plastic deformation of surface asperities, which breaks up the oxide film, producing relatively clean metal surfaces under intimate contact, establishing a metallurgical bond. After placing a layer, a computer controlled milling head shapes the layer to its slice contour. This milling can occur after each layer or, for certain geometries, after several layers have been deposited.

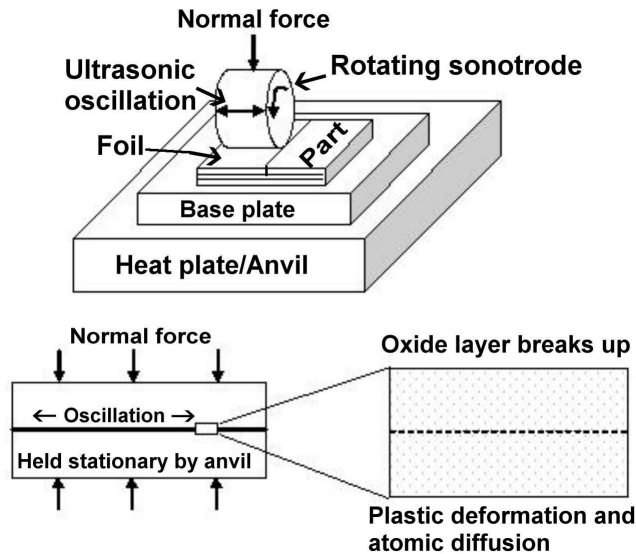


Fig.1. Schematic of the Ultrasonic Consolidation process.

One unique aspect of UC is that highly localized plastic flow around embedded structures is possible, resulting in sound physical/mechanical bonding between the embedded material and matrix material, although the exact mechanism by which it is made possible is not yet fully understood [4-6]. This makes the UC process a candidate fabrication method for fiber-reinforced metal matrix composites [3-5]. MMCs have traditionally been fabricated using diffusion bonding, casting or powder metallurgy techniques. Long-fiber or continuous fiber reinforced MMCs are mainly produced by diffusion bonding or spray deposition techniques, whereas short-fiber or discontinuous fiber reinforced MMCs are typically produced by powder metallurgy techniques [7]. Some of the disadvantages of these processes are: i) elevated processing temperatures, ii) high cost of tooling, and iii) limitations on geometrical shape.

In contrast, UC processing does not involve high temperatures. Although temperatures can reach up to 50% of the material melting point at the interface due to frictional heating [8], heat built up on the bulk part is practically negligible. Also, UC combines the advantages of additive and subtractive fabrication approaches allowing complex 3D parts to be formed with high dimensional accuracy and surface finish, including objects with complex internal passageways, objects made up of multiple materials, and objects integrated with wiring, fiber optics, sensors and instruments. Because the process does not involve melting, one need not worry about dimensional errors due to shrinkage, residual stresses and distortion in the finished parts. This will also help overcome the problems of brittle intermetallic formation and immiscibility while dealing with metallurgically incompatible dissimilar material combinations.

The UC process has been successfully used for fabrication of parts in various Al alloys [4,9,10]. Kong et al. have successfully embedded shape memory alloy (SMA) fibers in an Al 3003 matrix using the UC process [5], broadly demonstrating the process capability for manufacture of continuous fiber-reinforced MMCs. However, metal matrix composites intended for structural applications typically incorporate ceramic fibers (for example, SiC), and the results of their work cannot be directly applied to embedment of ceramic fibers in metal matrices because of the widely different physical, chemical, mechanical and thermal characteristics. No attempts have been reported in open literature on the use of ultrasonic consolidation process for manufacture of ceramic fiber reinforced metal matrix composites. Further, in their study, Kong et al [4,10] have not evaluated the effect of substrate temperature and fiber orientation with respect to welding direction on fiber embedding characteristics. These two aspects are expected to play a dominant role in ultrasonic consolidation of MMCs. Substrate temperature is important because it can strongly influence the plastic deformation process at the interface, which is considered to be the basic mechanism of bond formation during ultrasonic welding of metals [4]. It is necessary to understand the effect of fiber orientation on bond formation as, during actual part fabrication, it is necessary to change fiber orientation with respect to part axes in order to ensure isotropic properties.

In view of the above, the current work has been undertaken to explore the possibility of manufacturing SiC fiber reinforced Al matrix composites using the UC process. Specific objectives of this study include: i) identifying optimum combinations of process parameters, including substrate temperature and fiber orientation, and ii) evaluating fiber/matrix bond quality.

## **2. Experimental Work**

### **2.1 Materials and Sample Fabrication**

The metallic matrix material used in this study was Al alloy 3003 (nominal composition by wt.%, Al-1.2Mn-0.12Cu) foil, 150  $\mu\text{m}$  thick and 25 mm wide, obtained from Solidica, Inc., USA. Deposition experiments were conducted on an Al 3003 base plate (dimensions: 175x175x12 mm) firmly bolted to the heated platen in the machine. Silicon carbide fibers of 100 $\mu\text{m}$  diameter were used to produce MMCs. The SiC fiber consisted of a tungsten core (10 $\mu\text{m}$  diameter) and contained a 1  $\mu\text{m}$  thick pyrolytic carbon coating on the outer surface.

A design of experiments (DOE) approach was adopted to statistically evaluate the effect of process parameters on fiber/matrix bonding. A Taguchi L25 orthogonal array was utilized for this purpose. The process parameters and their levels chosen for this study are shown in Table 1. Variation of each parameter at five different levels was considered necessary to assess any non-linear effects. The levels for each of the process parameters were selected based on preliminary experiments, available literature [4,6,9,10] and machine-related considerations. Table 2 lists all the parameter combinations used for making the MMC deposits. MMC deposits of 100 mm long were made for all the 25 parameter combinations (hereafter identified by run numbers). The experiments were conducted in a randomized order and each run was repeated three times. The deposition

procedure consisted of (Fig.2): i) depositing a layer of Al 3003 on top of the Al alloy 3003 base plate, ii) placing a SiC fiber on the top of the deposited Al 3003 layer and holding it in place using a custom-designed fixture, and iii) depositing a layer of Al alloy 3003 on the pre-placed fiber. Thus three samples were obtained for each combination of parameters, and each sample was made of two layers of foils and a fiber embedded between them.

Table 1. Process parameters and their levels selected for UC experiments.

Parameter	Level 1	Level 2	Level 3	Level 4	Level 5
Oscillation amplitude ( $\mu\text{m}$ )	10	12.5	15	17.5	20
Welding speed (in/min)	60	70	80	90	100
Normal force (N)	1400	1550	1700	1850	2000
Temperature ( $^{\circ}\text{F}$ )	150	200	250	300	350
Fiber orientation $\dagger$ ( $^{\circ}$ )	0	30	45	60	90

$\dagger$   $0^{\circ}$  of fiber orientation is parallel to the sonotrode traveling direction, and  $90^{\circ}$  is perpendicular to the sonotrode traveling direction.

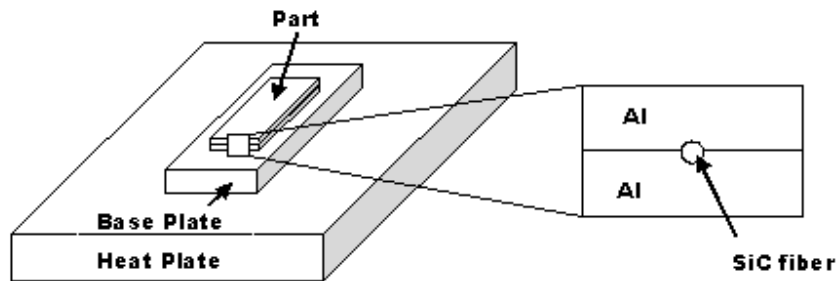


Fig.2. Schematic of the MMC deposit.

Table 2. Taguchi L25 experimental matrix along with corresponding push-out test results.

Run #	Amplitude ( $\mu\text{m}$ )	Speed (in/min)	Force (N)	Temp. ( $^{\circ}\text{F}$ )	Fiber orientation( $^{\circ}$ )	Debonding load (gf)		
						Sample 1	Sample 2	Sample 3
3	10	60	1400	150	0	235	-	-
7	10	70	1550	200	30	-	340	-
23	10	80	1700	250	45	682	738	773
10	10	90	1850	300	60	-	-	337
20	10	100	2000	350	90	-	-	-
9	12.5	60	1550	250	60	459	571	449
14	12.5	70	1700	300	90	552	600	558
18	12.5	80	1850	350	0	688	-	446
4	12.5	90	2000	150	30	-	-	-
22	12.5	100	1400	200	45	541	612	600
19	15	60	1700	350	30	234	658	609
21	15	70	1850	150	45	-	-	535
2	15	80	2000	200	60	344	493	-
13	15	90	1400	250	90	759	747	537
16	15	100	1550	300	0	513	382	546
6	17.5	60	1850	200	90	-	-	337
11	17.5	70	2000	250	0	-	-	333
15	17.5	80	1400	300	30	728	752	706
25	17.5	90	1550	350	45	682	-	697
1	17.5	100	1700	150	60	634	531	565
24	20	60	2000	300	45	914	750	789
17	20	70	1400	350	60	489	751	573
5	20	80	1550	150	90	743	642	697
8	20	90	1700	200	0	299	425	310
12	20	100	1850	250	30	409	362	394

## 2.2 Push-out Tests

In order to evaluate the fiber/matrix bond strength, a special test, termed push-out test, was used. The test involved pushing the fiber out of the matrix using a microhardness tester. Samples for these tests were prepared in the following way. Initially, around 1 mm thick slices containing the fiber region were extracted from each of the MMC deposits using a low speed diamond saw. These slices were mechanically polished using emery papers to produce a flat and even surface. This was followed by locally etching the tungsten core at the centre of the SiC fiber (using a solution consisting of 15mL HNO<sub>3</sub>, 3mL HF and 80mL H<sub>2</sub>O) in order to produce a small depression for the microhardness indenter to sit in. This etch procedure was found helpful in preventing sliding of the indenter during the push-out test. Push-out tests were performed using an Antonik microhardness tester, which has maximum load capacity of 1 kgf.

The push-out test was monitored by synchronizing a force sensor and an acoustic emission (AE) sensor. The load cell recorded the loading history while the AE sensor detected the initiation of debonding between fiber and metal matrix. The load at which debonding occurred was observed by tracing both the loading and acoustic emission signal history. The AE sensor selected for this study has a frequency response of 600 kHz, which is suitable for detecting cracking/debonding related signals in a normal environment [11]. After a 60dB total amplification, AE signals were recorded on a digital oscilloscope along with the loading information. Using this data, acoustic emission signals were plotted as a function of loading force. The force value recorded at the instance when the first negative spike occurred on the AE signal plot was taken as the threshold force required to cause fiber debonding, which is indicative of the fiber/matrix bond strength.

### **2.3 Microstructural studies**

All the MMC deposits were metallographically examined to assess the fiber/matrix bond quality. Samples corresponding to transverse sections (perpendicular to fiber direction) were extracted from each of the deposits and were prepared for microstructural study following standard metallographic practices. Microstructural observations were conducted on as-polished samples using a scanning electron microscope.

## **3. Results and Discussions**

### **3.1 Microstructures**

For successful embedment of fibers, there must be adequate plastic flow of the matrix material to close the gaps that were created by placing the fiber between the layers. The SiC fiber was found to embed well in the Al alloy 3003 matrix in all the experimental MMC deposits, as can be seen from the microstructures of one of the experimental deposits (Run # 5). It was observed that in all the deposits, the top and bottom Al 3003 layer were very well bonded in the vicinity of the fiber, although a few unbonded regions were always present at regions away from the fiber (Fig.3a). There is extensive plastic flow around the fiber, evidenced by flow lines in a circular pattern around the fiber (Fig.3a and 3b), resulting in excellent fiber embedment. The fiber/matrix interface looked tight without any large physical discontinuities in all the deposits (Fig.3c).

Studies thus show that SiC fibers can be successfully embedded in an Al 3003 matrix, making UC a viable process for fabrication of intricate parts out of continuous fiber reinforced metal matrix composites. Similar success was reported earlier by Kong et al. with shape memory alloy fibers in Al 3003 matrix [4,5]. The authors, through detailed elemental mapping studies, concluded that the matrix and the embedded fiber were not chemically or metallurgically bonded. Similarly in the present case, bonding between SiC fiber and Al 3003 matrix is expected to be physical/mechanical, rather than chemical/metallurgical.

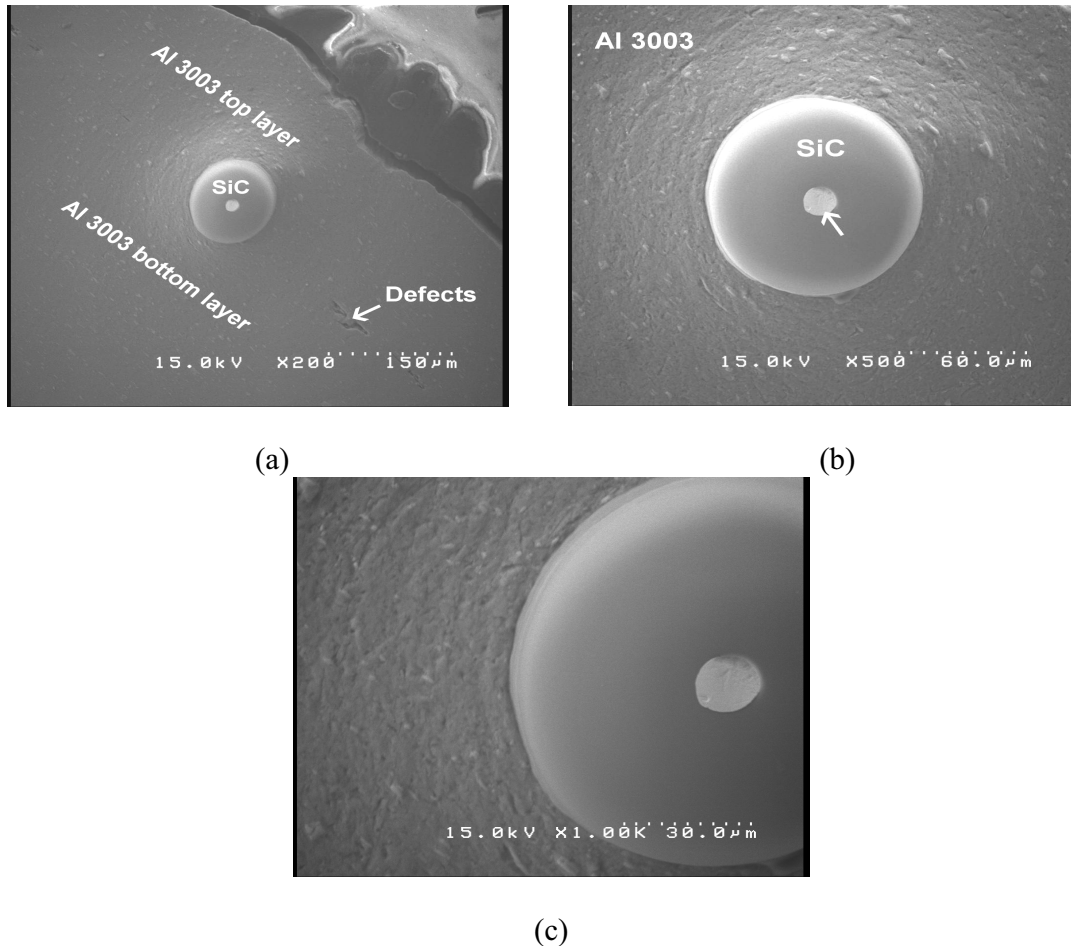


Fig.3. SEM images of Run #5 deposit: (a) X200, (b) X500, (c) X 1.00k.

### 3.2 Fiber/Matrix Bond Strength

The fiber/matrix bond strength was characterized by push-out tests as indicated in Section 2.2. The AE sensor used in this study was found to facilitate satisfactory observation of the fiber/matrix debonding event. A typical AE sensor signal vs. time plot obtained during the fiber push-out test (indentation on fiber) is shown in Fig.4a. Superimposed on the AE signal vs. time plot (red) is the load vs. time plot (blue). In most cases, the AE signal was found to rise (positive spike) and fall back to the background level and sometimes below the background level (negative spike) for more than one time while the applied load is increasing. Most of the AE signal vs. time plots showed a single sharp maximum negative spike, immediately following a positive spike. All these events occurred before the applied load reached its maximum value. After the load reached its maximum value, the AE signal generally remained at the background level with occasional positive/negative spikes, which correspond to small downward sliding movements of the fiber under the influence of the applied load. After the load was removed, a final positive spike was observed in most cases. This final positive spike can be ascribed to a reverse movement of the fiber due to elastic effects at the fiber/matrix

interface. David Marshall [12], who developed the fiber push-out test method, also noticed this reverse sliding of fiber during his studies on fiber-reinforced ceramic composites. In contrast, during microhardness indentation on the matrix material no such positive or negative spikes were observed, as can be seen from Fig.4b.

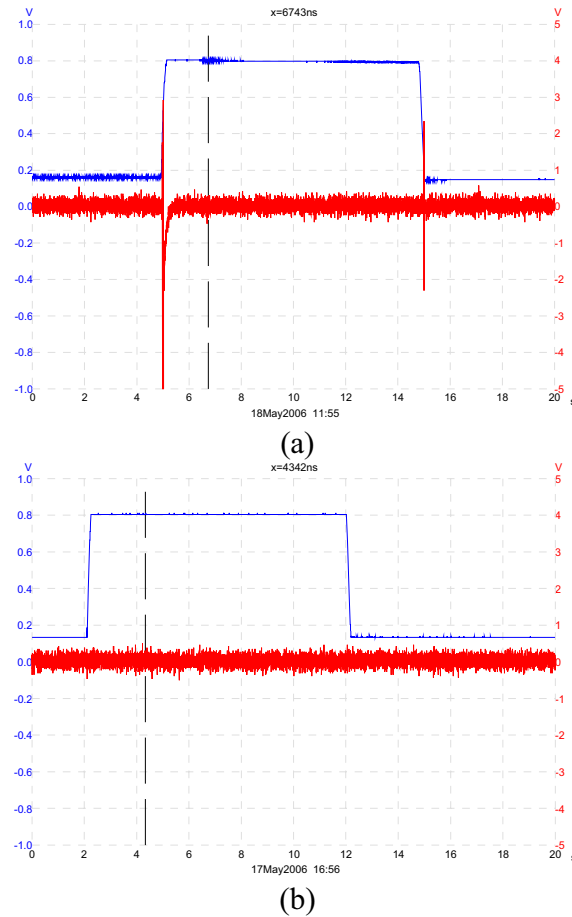


Fig.4. AE signal (red) and load (blue) plotted as a function of time during push-out test: (a) Indentation on fiber (Run #1), (b) Indentation on matrix material.

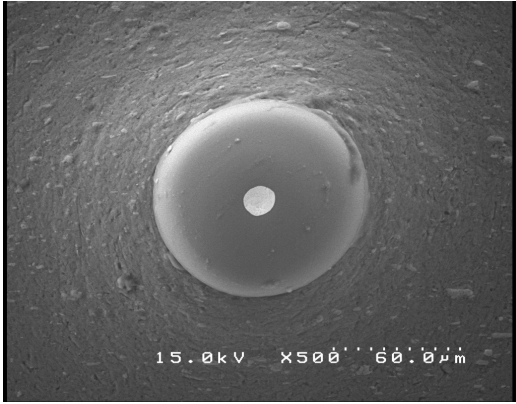
While it may appear logical to identify the time of debonding from one of the positive spikes, preferably from the first, our experience showed that the sharp maximum negative spike was a more reliable indicator of the debonding event. Debonding load values measured from the first positive spike were found to be inconsistent and random. While the reasons for this are not very clear, it is suspected that sliding or skidding of the indenter on the fiber as the applied load is increasing can result in such spurious positive spikes. Thus, the reported debonding loads in this study were measured from synchronized plots of AE signal vs. time and load vs. time plots, taking the time of maximum negative spike as the time of initiation of fiber/matrix debonding.



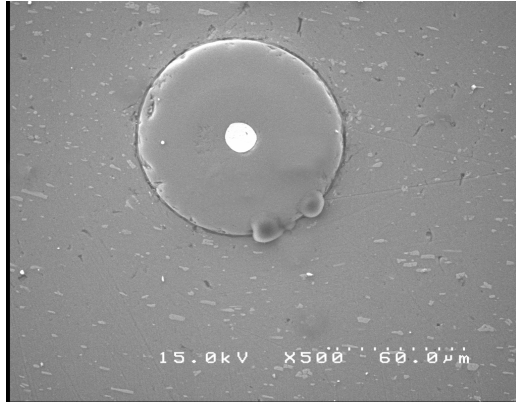
Following the procedure mentioned above, debonding loads were measured for all the 75 MMC deposits (25 experimental runs, each repeated three times), which are presented in Table 2. Debonding loads for some of the samples could not be measured as the samples debonded during sample preparation itself due to an extreme lack of bonding between the Al 3003 layers (for example, Run # 4 (all three samples), and Run # 21 (two samples)). The debonding load value in these cases was identified as “-”. Except for Run # 4 and Run # 20, at least one valid test result was available.

### **3.3. Bond Strength-Microstructure Correlations**

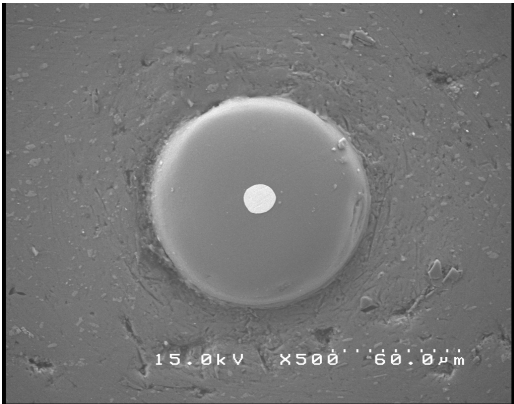
As can be seen from Table 2, the debonding load levels were found to vary significantly among the various experimental runs. However, debonding loads measured for the three samples of a given experimental run are reasonably consistent, except in cases where sample peel-off occurred. The SEM microstructures of the MMC deposits corresponding to various bond strength levels are shown in Fig.5. As can be seen, there was no obvious correlation of microstructural features with the observed variation in push-out test results among the various experimental runs. All the deposit showed good fiber embedment with sound metal flow around the fiber and there were no gross defects at the fiber/matrix interface. It is interesting to note that only some of the 25 runs showed distinct flow lines in a circular pattern around the fiber (for example, Run # 3, 5, and 7). This is likely due to the fiber orientation with respect to the rolled grain structure of the Al foil. However, the occurrence of distinct flow lines or lack thereof appears to have no direct correlation with the observed bond strength levels. For instance, Run # 3, 5 and 7, all with distinct flow lines, showed a wide variation in debonding loads (respective debonding loads were 235 gf, 678 gf, and 340 gf). Similarly, Run # 2, 13, and 21, all without distinct flow lines, also showed a wide variation in debonding loads (respective debonding loads were 405 gf, 281 gf, and 535 gf). Further, while some of the deposits with a low debonding force (Run # 12) showed some clearly discernible narrow physical discontinuities at the fiber/matrix interface, other samples (for example, Run # 3) with similar or even lower bond strength levels did not show the same and their microstructures, in fact, appeared as good as those with a high bond strength level. Thus, the current work could not establish a clear correlation between microstructural features and bond strength levels of the MMC deposits, making it necessary to examine the microstructures in greater detail at some future date.



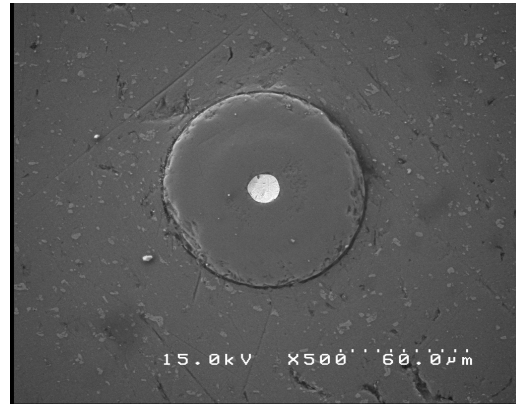
(a)



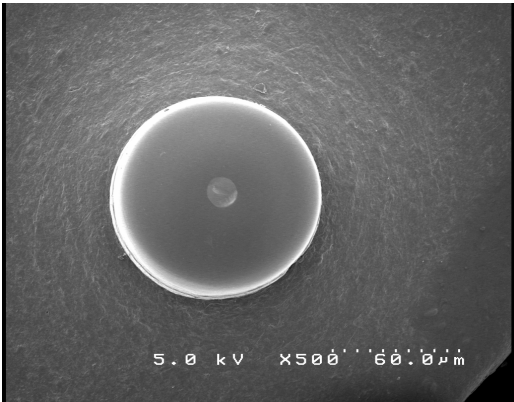
(b)



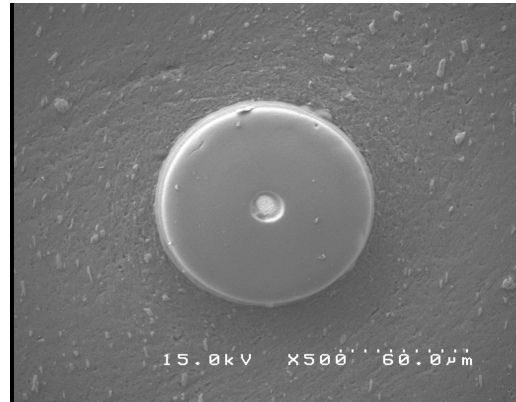
(c)



(d)



(e)



(f)

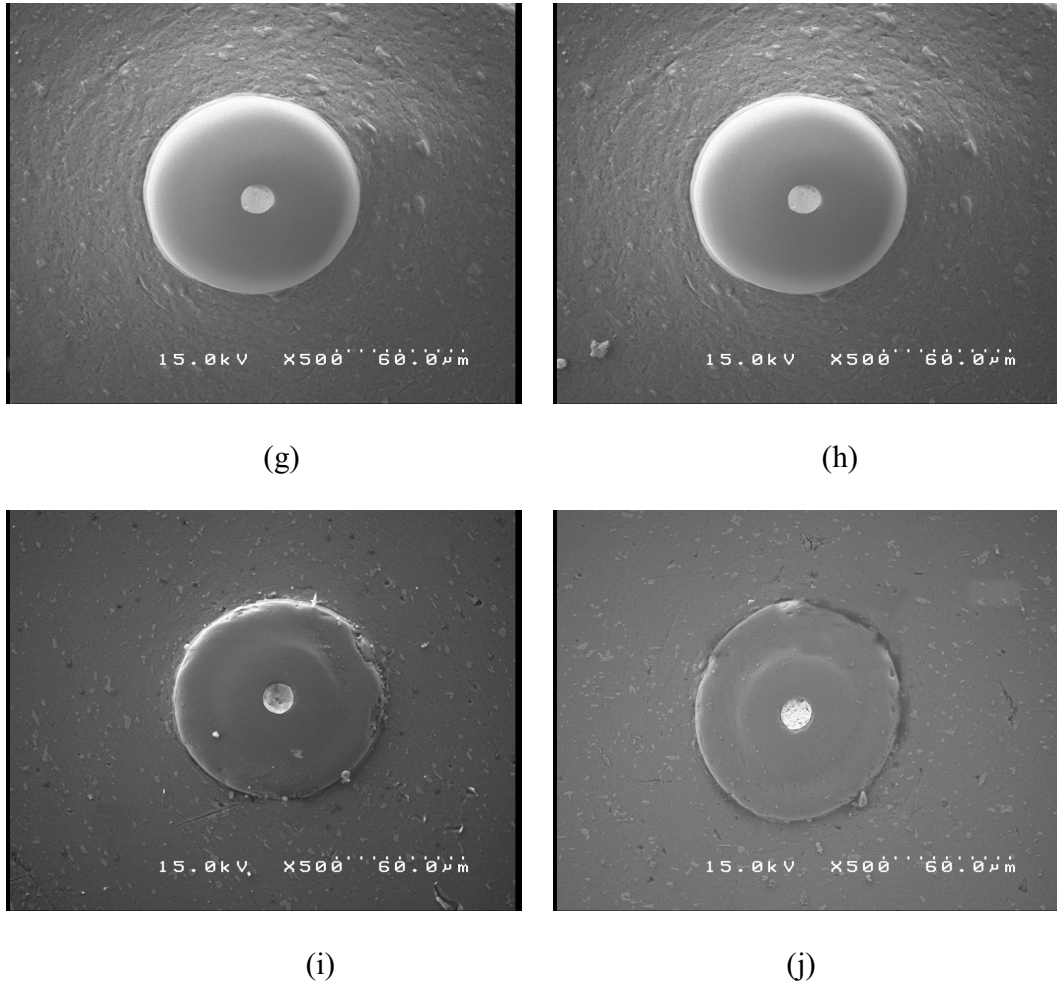


Fig.5. SEM microstructures of MMC deposits: (a) Run #3 (235 gf) (b) Run #13 (281 gf), (c) Run #19 (297 gf), (d) Run #12 (332 gf), (e) Run #7 (340 gf), (f) Run #2 (405 gf), (g) Run #21 (535 gf), (h) Run #5 (678 gf), (i) Run #15 (721 gf), (j) Run #24 (881 gf). All images are of X500. Values in brackets are the respective average debonding loads.

### 3.4. Effect of process parameters

#### 3.4.1 Statistical analysis

The debonding loads were found to change significantly among the experimental runs, ranging from 234 gf (Run # 19) to 914 gf (Run # 24), which indicates that the debonding load is strongly dependent on the process parameters. Analysis of variances (ANOVA) was performed to statistically evaluate the effect of each parameter on fiber/matrix bonding strength, following standard statistical procedures [13]. The results of ANOVA are summarized in Table 3 and Table 4. As can be seen, all the parameters have a statistically significant influence on bond strength at the 99% confidence level. Fiber orientation has the strongest effect on fiber/matrix bond strength among the five parameters studied in this investigation. Oscillating amplitude was found to be the second

most effective parameter. Normal force and welding speed were found have similar levels of influence on debonding load. Substrate temperature was found to have the weakest influence on bond strength among the five process parameters evaluated in the current study.

Table 3. Results of ANOVA analysis.

Source	Sums of squares (SS)	Degrees of freedom (v)	Variance (V)	F
Amplitude	4	223324	55831	28.11
Force	4	207061	51765	26.06
Speed	4	164061	41015	20.65
Temperature	4	140540	35135	17.69
Fiber Orientation	4	287205	71801	36.15
Residual Error	54	107268	1986	
Total	74	1129459		
F <sub>(table, 4,54)</sub> at 99% confidence $\approx 3.7$				

Table 4. Response table for means.

Level	Amplitude	Speed	Force	Temperature	Fiber Orientation
<b>1</b>	305	453	543	385	368
<b>2</b>	443	476	539	405	391
<b>3</b>	523	628	544	525	672
<b>4</b>	533	410	433	587	486
<b>5</b>	570	406	314	472	456
<b>Delta</b>	265	222	231	202	304
<b>Rank</b>	<b>2</b>	<b>4</b>	<b>3</b>	<b>5</b>	<b>1</b>

The effects of individual process parameters on fiber/matrix bond strength are graphically shown in Fig.6. It should be noted that the debonding load for each level of a particular parameter in Fig.6 corresponds to an average of five experimental runs at that level, with 3 replicates. The effects of each process parameter are discussed below in detail.

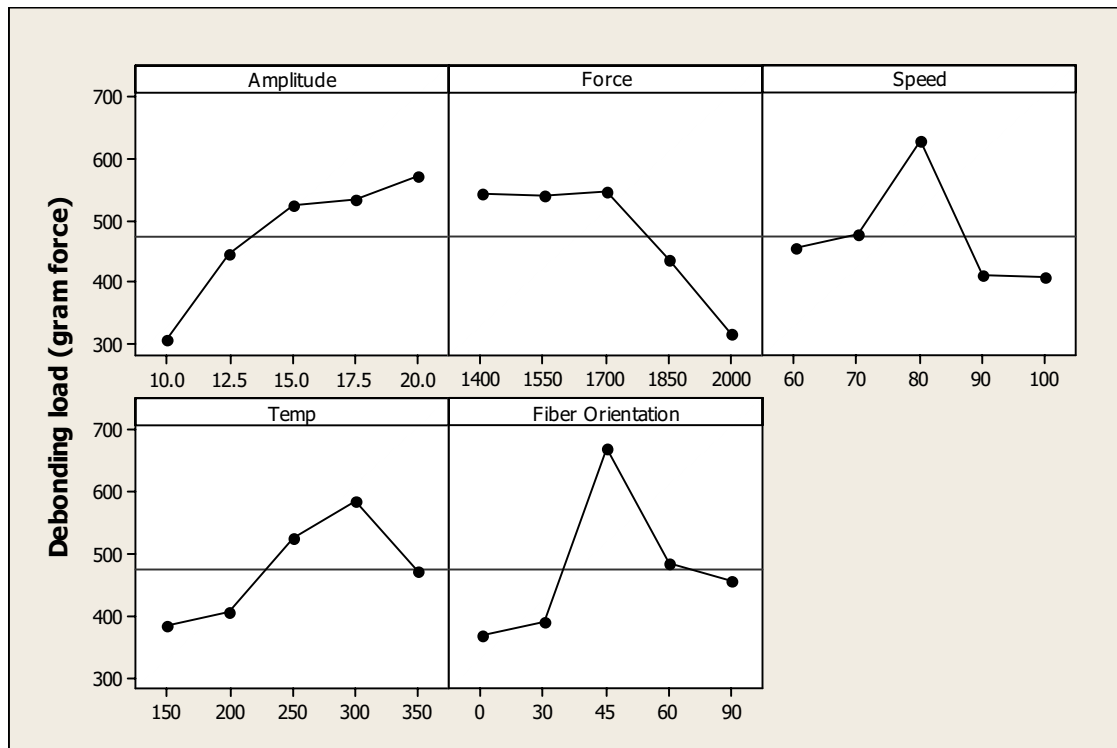


Fig.6. Effect of process parameters on debonding load.

### 3.4.2 Effects of oscillating amplitude

As mentioned above oscillating amplitude is the second most significant factor for fiber/matrix bond strength. It has a relatively linear effect on bond strength as can be seen in Fig.6. The average debonding load was found to increase from 305 gf to 570 gf with increase in oscillating amplitude from 10.0  $\mu\text{m}$  to 20.0  $\mu\text{m}$ . At a particular oscillation frequency, the higher the oscillation amplitude the higher would be the amount of applied ultrasonic energy into the system. This energy together with the static applied normal force determines the total energy available for weld formation. Therefore, an increase in oscillation amplitude increases the magnitude of oscillating shear forces and, hence, the magnitude of dynamic interfacial stresses at the interface between the two mating surfaces. This would enhance the elastic-plastic deformation at the surface contact points and facilitate easier removal of surface oxide layers and sound plastic flow around the fiber. It is likely for these reasons the deposits showed an increase in fiber/matrix bond strength with increase in oscillation amplitude from 10 to 20  $\mu\text{m}$ .

Kong et al. [9] observed similar improvements in bond strength with increasing oscillating amplitude in ultrasonically welded Al alloy 3003 foils. However, they observed a drop in bond strength, determined using peel-off testing, after a certain value of amplitude. Similarly, Janaki Ram et al. [14] reported a slight decrease in linear weld density in ultrasonically consolidated Al 3003 structures when the oscillation amplitude was increased beyond a certain level. The authors have ascribed this behaviour to generation of microcracks as well as strain hardening and fatigue related effects at the interface as a

result of excessive ultrasonic energy input [9,14]. In the present case, however, such non-linear effects of oscillation amplitude were not observed and the best results were obtained at an amplitude of 20  $\mu\text{m}$ .

### **3.4.3 Effects of normal force**

As shown in Fig.6, increase in normal force from 1400 N to 1700 N did not result in any change in debonding load, with a deviation less than 1%. However, further increases in normal force resulted in a considerable drop in debonding load, from an average value of 433 gf at 1700 N to 314 gf at 2000 N. Similar observations were reported by Kong et al. [9] and Janaki Ram et al. [14] during ultrasonic consolidation of Al alloy 3003. While the exact reason for this behavior is not clear at present, there are several potential explanations. As discussed previously, use of too high a normal force might result in excessive interfacial stresses leading to breakage of already formed bonds. Also, an increase in normal force will necessitate an increased sonotrode oscillatory force to maintain the same frequency. Excessive normal force might reduce the ability of the sonotrode to vibrate at its optimum frequency or set amplitude, thus leading to an overall reduction in operational performance and plastic flow at the interface. Another possible explanation is that when the normal force is high enough to create a stress state above the yield point of the material around the fiber, which, when released, can put the interface into tension weakening the interface. While further studies are necessary to fully assess the role of normal force during bond formation, the best results were obtained at an applied normal force of 1700 N in the present investigation. Thus too high a normal force was not desirable for SiC fiber embedding into an Al 3003 metal matrix.

### **3.4.4 Effects of substrate temperature**

Substrate temperature was found to have a nonlinear affect on fiber/matrix bond strength. As can be seen in Fig.6, an increase in substrate temperature from 150°F to 300°F resulted in an increase in fiber/matrix bond strength; however, a further increase in substrate temperature to 350°F, resulted in a considerable drop in bond strength. During ultrasonic welding, the in-situ raise in interface temperature as a result of friction plays a key role in bond formation by (i) reducing the flow stress of the material, (ii) enhancing atomic diffusion, and (iii) increasing the driving force for recrystallization [8]. In addition, any strain hardening effect during plastic deformation would be reduced at elevated temperatures. Use of external thermal energy input in the form of elevated substrate temperature would further enhance these effects and thus promote bond formation during ultrasonic welding. This explains why the fiber/matrix bond strength increased with increasing substrate temperature up to 300°F. It is, however, not clear why bond strength came down with further increase in substrate temperature. It is suspected that too high a substrate temperature can result in oxidation of metal foils, which can affect the fiber/matrix bond quality. Also, since the SiC fiber used in this study contained a thin carbon coating, it is possible that this coating was oxidized and sublimated or that localized heating during processing resulted in aluminum carbide formation, which can occur at temperatures as low as 500°C [15]. Aluminum carbide is extremely brittle and can reduce the fiber/matrix bond strength significantly.

### **3.4.5 Effects of welding speed**

As can be seen in Fig.6, the fiber/matrix bond strength was found to be improved when the welding speed increased from 60 in/min to 80 in/min. The debonding load reached a maximum value of 628 gf when a MMC deposit was produced at a welding speed of 80 in/min. The average value of debonding load decreased when the welding speed further increased from 80 in/min to 100 in/min. Thus MMCs should be fabricated at an intermediate welding speed. Given a certain amount of energy input, welding speed determines amount of energy input/unit length or, in other words, the time over which energy is applied at any particular point along the sonotrode traveling direction during ultrasonic welding. Use of higher welding speeds actually reduces sonotrode resident times and hence does not facilitate transfer of sufficient welding energy. Consequently, the magnitude of shear stresses generated at the fiber/matrix interface will be insufficient to cause complete oxide layer removal and to induce adequate plastic deformation of matrix metal. This explains why the MMC deposits showed decrease in fiber/matrix bond strength with increase in welding speed from 80 in/min to 100 in/min.

The reasons for the drop of debonding load at low welding speed levels are unclear. Several potential explanations for this, however, follow. First, low welding speed is in essence a long sonotrode resident time at a particular point, which may destroy the already formed fiber/matrix bond by some fatigue mechanism, which results in a drop in bond strength. Another potential explanation is that long sonotrode resident times can enhance the friction-induced heat build-up along the fiber/matrix interface, thus resulting in a high temperature issue, as discussed in Section 3.4.4, which reduces the debonding load.

### **3.4.6 Effects of fiber orientation**

Fiber orientation was found to be the most important processing parameter in the current study. As can be seen in Fig.6, 45° resulted in the highest fiber/matrix bond strength. Debonding loads at other fiber orientation angles were found to be significantly smaller than the one at 45°. As mentioned in earlier sections, plastic deformation of matrix metal is an essential fiber/matrix bond formation mechanism. It dominates the debonding load of MMC deposits. During UC processing, the maximum shear stress occurs at an angle of 45° with respect to the sonotrode oscillating direction. Consequently the plastic deformation which occurs at 45° should be significantly larger than that at other angles. Thus the largest fiber/matrix bond strength was achieved when fibers were placed along the 45° direction.

## **4. Conclusions**

Ultrasonic Consolidation has been successfully applied to the embedment of SiC fibers into Al 3003 metal matrices. Bond strength between the embedded SiC fibers and the Al 3003 metal matrix was found to be strongly dependent on process parameters. Variations in oscillation amplitude, welding speed, normal force, substrate temperature, and fiber orientation contribute to statistically significant variations in fiber/matrix debonding load. It was found that a push-out test using a microhardness indenter coupled with an acoustic emission sensor was a practical method to evaluate the fiber/matrix bond strength of MMCs, giving statistically significant variations amongst different parameter

sets. Using the Taguchi method and ANOVA, the following combination of parameters was found to produce the best fiber/matrix bond strength amongst the parameters tested: oscillation amplitude – 20  $\mu\text{m}$ , welding speed – 80 in/min, normal force – 1700 N, substrate temperature – 300°F, and fiber orientation – 45°.

Metal plastic deformation appears to be the essential mechanism for fiber/matrix bond formation. The fiber/matrix bond is expected to be physical/mechanical, rather than chemical/metallurgical.

## Reference

- [1] N. E. Weare, J. N. Antonevich, R. E. Monroe, Fundamental Studies of Ultrasonic Welding, *Welding Journal*, 39 (1960), 331s-341s.
- [2] H. P. C. Daniels, Ultrasonic welding, *Ultrasonics*, 3 (1965), 190-196.
- [3] Dawn R. White, Ultrasonic Consolidation of Aluminum Tools, *Advance Material & Processes*, 161 (2003), 64-65.
- [4] Choon Yen Kong, Investigation of Ultrasonic Consolidation for Embedding Active/Passive Fibers in Aluminum Matrices, *Doctoral thesis*, Loughborough University, May 2005.
- [5] C.Y. Kong, R.C. Soar, and P.M. Dickens, Ultrasonic consolidation for embedding SMA fibres within aluminium matrices, *Composite Structures*, 66 (2005), 421-427.
- [6] C. Domanidis and Y. Gao, Mechanical modeling of ultrasonic welding, *Welding Journal*, April, 83 (2004), 140s-146s.
- [7] T. W. Clyne, P. J. Withers, An introduction to metal matrix composites, Cambridge University Press, Cambridge, 1993.
- [8] O'Brien, R.L., Welding Processes, *Welding Handbook*, Vol. 2, 8<sup>th</sup> ed., American Welding Society, Miami, 783 (1991).
- [9] C. Y. Kong, R.C. Soar, P.M. Dickens, Optimum process parameters for ultrasonic consolidation of 3003 aluminum, *Journal of material processing technology*, V 146 (2004) 181-187.
- [10] C.Y. Kong, R.C. Soar, and P.M. Dickens, Characterization of aluminium alloy 6061 for the ultrasonic consolidation process, *Materials Science and Engineering A*, 363 (2003), 99-106.
- [11] Richard Nordstrom, Introduction to AE and AE Instrumentation, Pre-conference Event for AEWG-46, Portland, Oregon, Aug. 4-6, 2003.
- [12] David B. Marshall, W. C. Oliver, Measurement of Interfacial Mechanical Properties in Fiber-reinforced Ceramic Composites, *J. Am. Ceram. Soc.*, 70 [8] 542-48 (1987).
- [13] Ranjit Roy, A primer on the Taguchi Method, Van Nostrand Reinhold, New York, 1990.
- [14] G.D. Janaki Ram, Y. Yang, and B.E. Stucker, Improving Linear Weld Density in Ultrasonically Consolidated Parts, Solid Freeform Fabrication Symposium, Austin, TX, 2006.
- [15] Sheng-han Li, Chuen-guang Chao, Effects of Carbon Fiber/Al Interface on Mechanical Properties of Carbon-Fiber-Reinforced Aluminum-Matrix Composites, *Metallurgical and Materials Transactions A*, 35A (2004), 2153-2160.